How far ahead could we predict El Niño?

Matthew Collins[1]
Centre for Global Atmospheric Modelling, Department of Meteorology, University of Reading, Reading, UK.

David Frame
Centre for Global Atmospheric Modelling, Dept. Meteorology, University of Reading, Reading, UK.

Bablu Sinha
Southampton Oceanography Centre, University of Southampton, Southampton, UK.

Chris Wilson
Oceanography Laboratories, University of Liverpool, Liverpool, UK.

Abstract.
The upper limit of the predictability of the El Niño Southern Oscillation (ENSO) is examined using ensembles of simulations of a coupled ocean-atmosphere global circulation model which has a relatively realistic ENSO cycle. By making small perturbations to the initial conditions and measuring the rate of divergence of nearby trajectories, it is found that given a perfect model and near perfect initial conditions, ENSO could be usefully predicted, on average, up to 8 months in advance (where "useful" is defined for a forecast with an anomaly correlation coefficient of greater than 0.6). This is at the low end of potential predictability estimates obtained using intermediate models. Some ensemble experiments do show potential predictability beyond 12 months, but in others small "errors" in the initial conditions can saturate in less than 6 months. The physical mechanisms which underlie the high and low predictable states are briefly examined with a view to predicting the reliability of ENSO forecasts.

Introduction

The El Niño Southern Oscillation (ENSO) involves a quasi-periodic warming and cooling of the Eastern Tropical Pacific sea surface, accompanied by corresponding changes in atmospheric circulation patterns. ENSO has a significant impact on world ecology, society and economics and there are currently international efforts to predict ENSO at seasonal lead times using both dynamical and statistical methods, both of which have met with considerable success (*Barnston et al.* [1999]). A typical dynamically-based ENSO forecast system involves assimilating observations into a coupled ocean-atmosphere model to produce an estimate of the current state of the system, and running the model forward in time to produce a forecast (often the model is run many times

to produce an ensemble - *Stockdale et al.* [1998]). In such a system, there are three principal ways in which the forecast can go wrong: (i) the observations (and the data assimilation scheme) may be insufficient to produce an accurate estimate of the initial ocean-atmosphere state; (ii) the model can be in error and; (iii) the system may be inherently unpredictable, such that infinitesimal errors in the initial conditions grow rapidly, i.e. the system exhibits sensitive dependence on initial conditions. The latter is of considerable importance as even if we could assimilate perfect observations into a perfect model, the lead time would be constrained by the chaotic nature of the system.

Method

ENSOs sensitive dependence on initial conditions can be isolated from other potential sources of error using a "perfect model" or "perfect ensemble" approach. Ensembles of the Hadley Centre Coupled Ocean Atmosphere model (HadCM3 - *Gordon et al.* [2000]) are performed with small perturbations to the atmospheric initial conditions, and the ensemble spread is examined as a function of lead-time to assess the potential predictability limit. HadCM3 is a non-flux-adjusted coupled model which simulates ENSO with an amplitude and period (of approximately 3-4 years) which is very similar to that observed (*Collins* [2001]). Hence the potential predictability limit for the model is likely to be close to that of the real system. The major advance in this study over previous potential predictability studies (*Goswami and Shukla* [1991], *Ineson and Davey* [1997], *Kirtman and Schopf* [1998], *Grotzner et al.* [1999], *Thompson and Battisti* [2000]) is that we utilize a fully coupled dynamical ocean-atmosphere model that (i) has a relatively realistic simulation of the ENSO cycle, and (ii) has a stable surface climatology which is achieved without the use of flux corrections which may effect predictability. The model explicitly simulates the dynamical complexity of both the ocean and the atmosphere; complexity which may significantly effect the predictability and may not be simulated in intermediate ENSO models.

We perturb the ensembles from the 4 experiments of *Stott et al.* [2000] which simulate much of the surface temperature variability of the 20th century on multi-decadal time scales by including estimates of both anthropogenic and natural factors which effect climate. The question of how to perturb atmospheric initial conditions has been one of considerable research effort with the development of singular vectors (*Molteni et al.* [1996]) and breeding vectors (*Toth and Kalnay* [1993]). While some progress has been made in applying similar methods to intermediate coupled models of the climate system (*Chen et al.* [1997]), here we use a more pragmatic approach. Because it is the ocean which is

the slowly varying component of the coupled system which may lead to predictability, and because the weather forecasting limit is on the order of a week or so, we simply fix the ocean initial state and take successive model days for the atmospheric initial states of the ensemble. Thus for each ensemble experiment the individual members have identical ocean initial conditions and atmospheric initial conditions which differ across the ensemble only by as much as the weather can change in one week. Because of limited computer resources we take ensembles of size 5 in this study, but perform experiments at various points on the "climate attractor" in order to build up a picture of potential ENSO predictability. While the number of experiments performed here is clearly lower than those studies which use intermediate ENSO models, they involve over 300 years of coupled GCM integration and thus represent the most comprehensive study of this kind to date.

Results

NINO3 anomalies (an index of ENSO activity) from such ensemble experiments are shown in fig. 1. Each set of experiments starts in December of the indicated year and is run for 5 years. What is first apparent is that simply by making relatively small perturbations to the atmospheric initial conditions there can be rapid divergence of the ensemble members, i.e. the system does appear to exhibit sensitive dependence on initial conditions. There is a richness of behaviour in these experiments which indicates a wide range of potential predictability. Ensembles d, e and l, for example, show that after one year the ensemble spread is essentially on the order of the climatological variability, indicating loss of predictability at this lead time. Other ensembles, for example b, g and h show relatively small ensemble spread out to 1 year and, in the case of g and h, the individual members appear to track each other for many years into the experiment. Ensemble k is unique in that none of the 5 members simulate a large ENSO event for the full 5 years of the experiment. Variability in the predictability of ENSO has been highlighted in ENSO forecasting studies which use intermediate complexity models (e.g. *Kirtman and Schopf* [1998]) and has been associated with decadal fluctuations in the climate of the Pacific region. This variability is confirmed by this study using a comprehensive coupled model.

fig. 1

We can summarize average potential ENSO predictability by producing statistics for all the ensemble experiments shown in fig. 1. The average anomaly correlation coefficient (ACC, fig. 2 (a)) shows a decrease in skill to zero after 18 months and subsequent random fluctuations around zero after this. The root mean square error (RMSE, fig. 2 (b)) shows a large seasonal cycle associated with the phase locking of maximum ENSO variance to Northern Hemisphere

fig. 2

winter, but shows error growth followed by saturation in agreement with the ACC. Forecast accuracy is ultimately defined by the user of the forecast, but taking a value of ACC of 0.6 to define a "useful" forecast accuracy (*Kirtman and Schopf* [1998]), then given a perfect model and near perfect initial conditions, ENSO would be predictable, on average, out to a lead time of 8 months. This limit is at the lower end of the range found in studies that use intermediate ENSO models (e.g. *Goswami and Shukla* [1991], *Kirtman and Schopf* [1998], *Thompson and Battisti* [2000]). Fitting the modified Lorenz forecast error growth model (*Dalcher and Kalnay* [1987]) to the RMSE we get a error growth rate of 0.19 $(\text{month})^{-1}$. This gives an error doubling time of around 3.6 months in comparison 4.5 months found by *Goswami and Shukla* [1991]. Thus the coupled GCM seems to show more rapid error growth and less potential predictability than the intermediate ENSO models.

The ACC for a persistence forecast (also shown in fig. 2 (a)) drops below 0.6 after 5 months and drops to zero at around 15 months lead time. Hence even with a perfect model and near-perfect initial conditions, the potential average gain in skill over a simple persistence forecast is only 3 months (although this gain maybe longer in the case of more predictable ENSO states).

Average statistics of predictability are somewhat misleading as there are cases where ensemble spread grows more rapidly or more slowly leading to shorter and longer potential lead times. Fig. 2 shows the ACC and RMSE for ensembles e, d and l which show more rapid ensemble spread and ensembles b, g and h in which the ensemble spread grows less rapidly. For the least predictable states, useful predictability (again defined by an ACC greater than 0.6) is only potentially possible out to a lead time of 6 months, whereas for the more predictable states the useful predictability limit may potentially be of the order of a year or greater. By examining the physical mechanisms responsible for setting these low and high predictability states, it may be possible to define pre-cursors that indicate when they might occur, and hence quantify, a priori, forecast accuracy.

High and low predictable states

Ensemble e (fig. 1) is a case of rapid ensemble spread in which 4 of the 5 ensemble members remain in neutral or weak El Niño conditions one year in, whereas one ensemble member has a strong El Niño event. The evolution of the thermocline in 3 of the ensemble members is shown in fig. 3. In all of the members there is a tilting of the thermocline in the first 6-7 months of the experiment towards weak El Niño conditions. In member 1, this subsequently dies out and the system returns to a neutral state. In member 2, a thermocline anomaly develops in mid-basin but persists only for a

fig. 3

few months and eventually recedes. In member 3, a similar but stronger mid-basin anomaly develops and during the Autumn season and there is some westerly wind activity in the west which then initiates a strong El Niño event. Hence in this ensemble there appears to be (at least) two mechanisms by which the system can be unpredictable. Firstly, there is some sensitive dependence on initial conditions which leads the ocean-atmosphere state to develop different thermocline states (member 1 and 2) and secondly, random atmospheric fluctuations can further perturb the system causing nearby trajectories to diverge (members 2 and 3). This hints that both deterministic chaos and stochastic forcing both play a role in determining the predictability characteristics of the model ENSO cycle (see also *Thompson and Battisti* [2000]).

There are two possible explanations for the potential predictability at an extended range (i.e. beyond the average 8 month lead time) shown in ensembles b, g and h: The relatively small divergence of ensembles members might be due to chance (because of the small ensemble size) or there may be some physical reason why ENSO is more predictable at this point of "the attractor". The latter is of considerable importance as identifying such pre-cursors to predictable states is crucial in assessing forecast reliability. Increasing the ensemble size in experiment g by adding 4 more members (fig. 4) broadens the ensemble spread initially, such that after one year the members range from neutral conditions to a strong El Niño. Thereafter one member diverges from the other 8 which all tend to indicate a weak La Nina followed by another El Niño event. Further addition of ensemble members would allow more probabilistic measures of potential predictability to be employed as they are in ensemble forecast verification (*Buizza et al.* [2000]), however it appears that the extended range potential predictability seen in ensemble g was, in fact, a statistical fluke. Real extended range predictability might occur when the system is far away from equilibrium, for example when the thermocline is raised over the entire equatorial basin indicating a lack of zonally averaged heat content which is subsequently recharged as part of a recharge-discharge cycle (*Jin* [1997]). This is indeed the case for ensembles b and h (table 1), although much more work is required in order to predict the reliability of ENSO forecasts.

fig. 4

table 1

Discussion

A known modulator of ENSO predictability is the time of year from which forecasts are initiated (*Latif et al.* [1998]). Due to limitations on computer time it has not been possible to examine this seasonal predictability dependence (all our ensemble experiments were started on 1st December). However it is expected that the predictability limit will be somewhat longer (of the order of a few months) for experi-

ments initiated during the boreal spring season (*Thompson and Battisti* [2000]). The spring predictability barrier can clearly be seen as discontinuities in the rate of change of the skill measures shown in fig. 2 in the first year of the experiments.

It is important to re-iterate that the predictability limit derived from this perfect model study is an upper bound on the predictability for any real forecasting system. We must further increase our ability to observe the ocean-atmosphere system, our ability to improve couple ocean-atmosphere models and our ability to successfully assimilate the observations into the model in order to improve ENSO forecasts.

Acknowledgements

This work was supported by the UK Natural Environmental Research Programme under the thematic programme - Couple Ocean Atmosphere Processes in European Climate and by the European Union Framework 5 programme under the PREDICATE project. We are grateful for the comments of one anonymous reviewer.

References

Barnston, A. G., Glanz, M. H. and He, Y. Predictive skill of statistical and dynamical climate models in forecasts of SST during the 1997-98 El Niño episode and the 1998 La Nina onset. *Bull. Amer. Met. Soc., 80*, 217-243, 1999.

Buizza, R., Barkmeijer, J., Palmer, T. N. and Richardson, D. S., Current status and future developments of the ECMWF ensemble prediction system. *Met. Apps., 7*, 163-175, 2000.

Chen, Y. Q., Battisti, D. S., Palmer, T. N., Barsugli, J. and Sarachik, E. S. A study of the predictability of tropical Pacific SST in a coupled ocean-atmosphere model using singular vector analysis: The role of the annual cycle and the ENSO cycle. *Mon. Wea. Rev., 125*, 831-845 1997.

Collins, M., Tett, S. F. B. and Cooper, C., The internal climate variability of HadCM3, a version of the Hadley Centre coupled model without flux adjustments. *Climate Dynamics, 17*, 61-81 2001.

Dalcher, A. and Kalnay, E., Error growth and predictability in operational ECMWF forecasts. *Tellus, 39A*, 474-491.

Gordon, C. et al., The Simulation of SST, sea ice extents and ocean heat transport in a version of the Hadley Centre coupled model without flux adjustments. *Climate Dynamics, 16*, 147-168 2000.

Goswami, B. N. and Shukla, J., Predictability of a coupled ocean-atmosphere model. *J. Climate, 4*, 3-22, 1991.

Grotzner, A., Latif, M., Timmermann, A. and Voss, R. Interannual to Decadal Predictability in a coupled ocean-

atmosphere general circulation model. *J. Climate, 12*, 2607-2624, 1999.

Ineson, S. and Davey, M. K. Interannual climate simulations and predictability in a coupled TOGA GCM. *Mon. Wea. Rev., 125*, 721-741, 1997.

Jin, F.-F. An equatorial ocean recharge paradigm for ENSO. Part I: Conceptual model. *J. Atmos. Sci., 54*, 811-829, 1997.

Kirtman, B. P. and Schopf, P. S., Decadal variability in ENSO predictability and prediction. *J. Climate, 11*, 2804-2822 1998.

Latif, M. et al. TOGA review paper: Predictability and Prediction. *J. Geophys. Res, 103*, 14375-14394 1998.

Molteni, F., Buzzia, R. and Palmer, T. N. The ECMWF ensemble prediction system: Methodology and validation. *Q. J. Roy. Met. Soc., 122*, 73-119 1996.

Stockdale, T. N., Anderson, D. L. T., Alves, J. O. S. and Balmaseda, M. A., Global seasonal rainfall forecasts using a coupled ocean-atmosphere model.*Nature, 392*, 1998.

Stott, P. A. et al., External control of 20th century temperature by natural and anthropogenic factors. *Science, 290*, 2133-2137 2000.

Thompson, C. J. and Battisti, D. S., A linear stochastic dynamical model of ENS0. Part II: Analysis. *J. Climate, 14*, 445-466 2000.

Toth, Z. and Kalnay, E. Ensemble forecasting at NMC: The generation of perturbations. *Bull. Amer. Met. Soc., 74*, 2317-2330 1993.

Table 1. The anomalous depth of the equatorial basin average thermocline (as measured by the depth of the 20°C isotherm averaged in the region 150E - 90W, 2S-2N) in the period September-November prior to the initialisation of the ensemble experiments shown in fig. 1. Ensembles b and h, which show potential predictability at extended lead times have anomalously shallow thermoclines prior to the start of the experiments. Figures in brackets are the anomalies expressed as multiples of the standard deviation of this quantity.

a	9.2m (0.89)	e	-11.5m (1.11)	l	-4.7m (0.46)
b	-24.9m (2.40)	f	10.0m (0.97)	j	-4.4m (0.43)
c	-1.1m (0.11)	g	-14.9m (1.44)	k	-7.8m (0.75)
d	7.0m (0.67)	h	-19.7m (1.90)	l	17.2m (1.66)

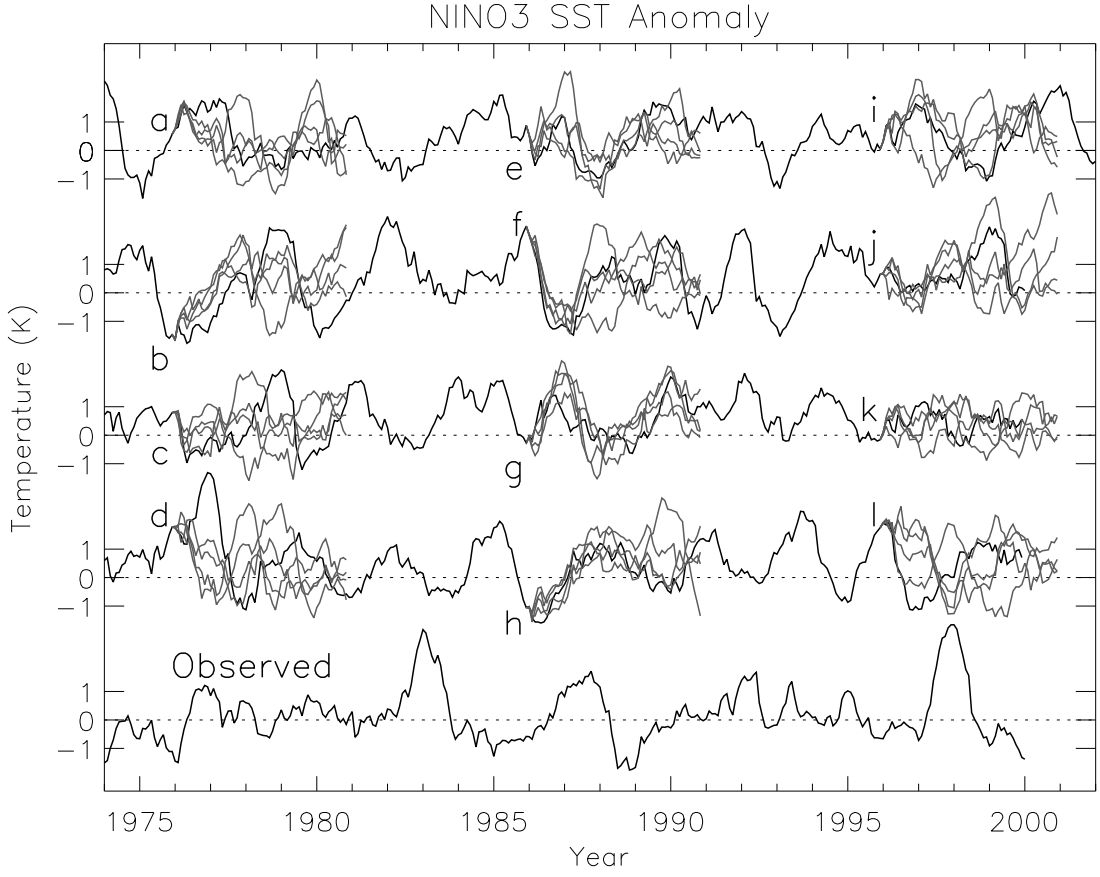

Figure 1. SST anomalies averaged in the NINO3 region (150W - 90W, 5S-5N) for the four coupled model realisations of 20th century climate (black lines) and the ensemble experiments (grey lines labelled a-l) which have small perturbations to the initial conditions (see text for more details). The rate of spread of the ensemble members gives an indication of the potential predictability of ENSO. The observed NINO3 anomalies are also shown to indicate the relative realism of the coupled model ENSO cycle.

Figure 1. SST anomalies averaged in the NINO3 region (150W - 90W, 5S-5N) for the four coupled model realisations of 20th century climate (black lines) and the ensemble experiments (grey lines labelled a-l) which have small perturbations to the initial conditions (see text for more details). The rate of spread of the ensemble members gives an indication of the potential predictability of ENSO. The observed NINO3 anomalies are also shown to indicate the relative realism of the coupled model ENSO cycle.

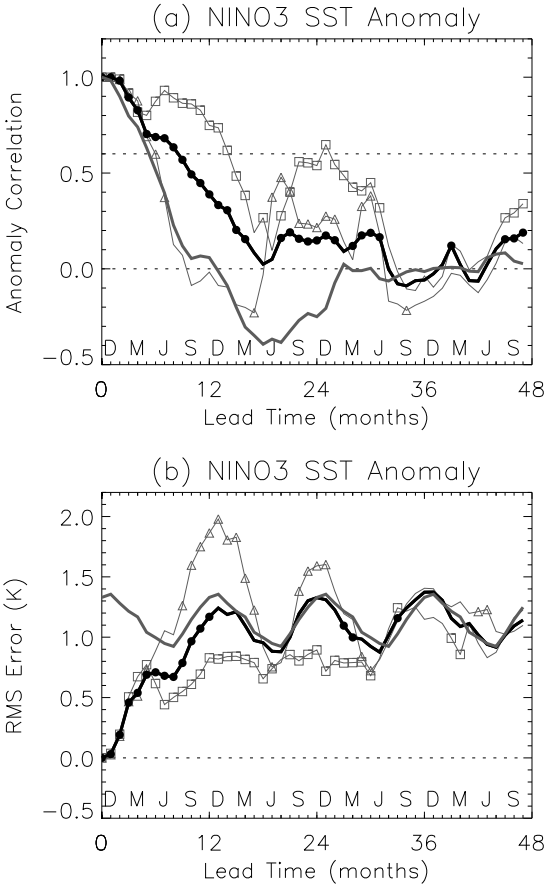

Figure 2. Measures of the potential predictability of ENSO, (a) anomaly correlation coefficient (ACC), and (b) root mean squared error (RMSE). In each the solid black line is the average computed for all the ensemble experiments shown in fig. 1. The thick grey line in (a) is the ACC computed for a persistence forecast and the thick grey line in (b) is the climatological RMS. Filled circles indicate statistical significance at greater that the 5% level for an ACC greater than zero or an RMSE greater or less than the climatological variability. The thin grey lines show the ACC and RMSE for the high (b, g, and h, with squares showing statistical significance) and low (d, e and l, with triangles showing statistical significance) predictability ensembles.

Figure 2. Measures of the potential predictability of ENSO, (a) anomaly correlation coefficient (ACC), and (b) root mean squared error (RMSE). In each the solid black line is the average computed for all the ensemble experiments shown in fig. 1. The thick grey line in (a) is the ACC computed for a persistence forecast and the thick grey line in (b) is the climatological RMS. Filled circles indicate statistical significance at greater that the 5% level for an ACC greater than zero or an RMSE greater or less than the climatological variability. The thin grey lines show the ACC and RMSE for the high (b, g, and h, with squares showing statistical significance) and low (d, e and l, with triangles showing statistical significance) predictability ensembles.

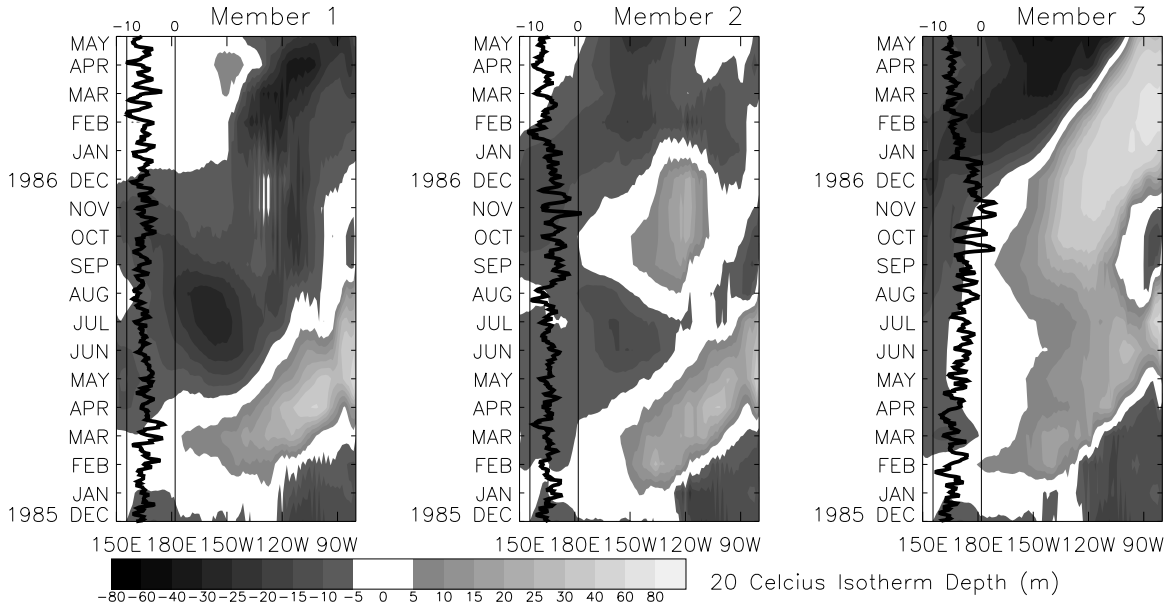

Figure 3. Longitude time maps of the anomalous depth of the 20C isotherm (an indicator of the depth of the thermocline) averaged between 2S and 2N for 3 of the ensemble members from experiment e. Member 3 is the ensemble member which executes a strong ENSO event while members 1 and 2 do not. On each panel the thick black line is the daily zonal wind averaged in the region bounded by the 2 thin vertical lines, with the scale indicated on the top axes in ms^{-2}. Positive values indicate an anomalously deep thermocline.

Figure 3. Longitude time maps of the anomalous depth of the 20C isotherm (an indicator of the depth of the thermocline) averaged between 2S and 2N for 3 of the ensemble members from experiment e. Member 3 is the ensemble member which executes a strong ENSO event while members 1 and 2 do not. On each panel the thick black line is the daily zonal wind averaged in the region bounded by the 2 thin vertical lines, with the scale indicated on the top axes in ms^{-2}. Positive values indicate an anomalously deep thermocline.

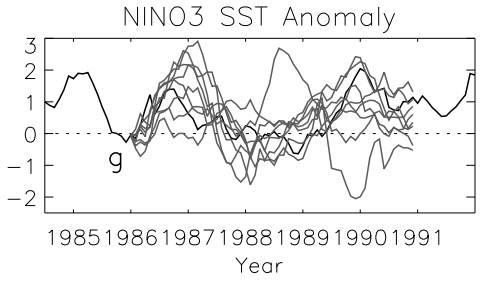

Figure 4. NINO3 anomalies for experiment g with an extra 4 ensemble members compared to that shown in fig. 1. By adding extra ensemble members in this case, the ensemble spread is increased and the estimate of potential predictability is correspondingly reduced.

Figure 4. NINO3 anomalies for experiment g with an extra 4 ensemble members compared to that shown in fig. 1. By adding extra ensemble members in this case, the ensemble spread is increased and the estimate of potential predictability is correspondingly reduced.

COLLINS: HOW FAR AHEAD COULD WE PREDICT EL NIÑO?

COLLINS: HOW FAR AHEAD COULD WE PREDICT EL NIÑO?